J Mater Sci: Mater Med (2008) 19:3319–3326
DOI 10.1007/s10856-008-3467-5

Zn^{2+} release behavior and surface characteristics of Zn/LDPE nanocomposites and ZnO/LDPE nanocomposites in simulated uterine solution

Zhihong Yang · Changsheng Xie · Xianping Xia · Shuizhou Cai

Received: 7 June 2007 / Accepted: 30 April 2008 / Published online: 22 May 2008

Abstract To decrease the side effects of the existing copper-bearing intrauterine devices, the zinc/low-density polyethylene (Zn/LDPE) nanocomposite and zinc-oxide/low-density polyethylene (ZnO/LDPE) nanocomposite have been developed in our research for intrauterine devices (IUDs). In this study, the influences of preparation methods of nanocomposites and particle sizes of zinc and zinc oxide on Zn^{2+} release from composites incubated in simulated uterine solution were investigated. All release profiles are biphasic: an initial rapid release phase is followed by a near zero-order release period. Zn^{2+} release rates of nanocomposites prepared by compressing moulding are higher than those of the nanocomposites prepared by hot-melt extrusing. Compared with Zn^{2+} release from the microcomposites, the release profiles of the nanocomposites exhibit a sharp decrease in Zn^{2+} release rate in the first 18 days, an early onset of the zero-order release period and a high release rate of Zn^{2+} at the later stage. The microstructure of the Zn/LDPE sample and the ZnO/LDPE sample after being incubated for 200 days was characterized by SEM, XRD and EDX techniques. The results show that the dissolution depth of ZnO/LDPE nanocomposite is about 60 μm. Lots of pores were formed on the surface of the Zn/LDPE sample and ZnO/LDPE sample, indicating that these pores can provide channels for the dissolution of nanoparticles in the matrix. The undesirable deposits that are composed of ZnO are only detected on the surface of Zn/LDPE nanocomposite, which may increase the risk of side effects associated with IUDs. It can be expected that ZnO/LDPE nanocomposite is more suitable for IUDs than Zn/LDPE nanocomposite.

Z. Yang
Faculty of Material Science and Chemical Engineering, China University of Geosciences, Wuhan 430074, People's Republic of China

Z. Yang · C. Xie (✉) · X. Xia · S. Cai
State Key Laboratory of Material Processing and Die & Mould Technology, Department of Materials Science and Engineering, Huazhong University of Science and Technology, Wuhan, Hubei 430074, People's Republic of China
e-mail: csxie@mail.hust.edu.cn

1 Introduction

The intrauterine devices (IUDs) are the most widely used reversible method of contraception in the world today. However, after Cu-IUDs insertion, some side effects such as pelvic inflammatory disease [1, 2], pain and bleeding [3, 4] have been observed by some researchers. Although some improvements have been achieved, concerns about side effects remain stubborn obstacles to a wider use of modern IUDs. Therefore, the goal of the IUDs design and innovation is still to decrease the side effects without sacrificing contraceptive effectiveness.

One possible way to solve the problem of side effects is the addition of zinc in Cu-IUDs. Free zinc (Zn^{2+}) not only plays an important role in the process of development, cell division and the synthesis of proteins and DNA, but also helps wound healing and tissue repair of the endometrium [5, 6], implying that it may reduce the incidence of pain and bleeding by healing the uterus injury caused by IUDs insertion. Moreover, zinc can help to prevent the risk of pelvic inflammatory disease because zinc ions have been found to have antibacterial effects on some microbes [7, 8]. However, level of zinc in endometrium and cervical mucus decreases after the insertion of Cu-IUDs [9, 10]. It has been reported that one of the important factors that cause side

effects after Cu-IUDs insertion is the absence of free zinc. Therefore, such side effects as pain, bleeding and pelvic inflammatory disease might decrease after zinc is introduced into Cu-IUDs, which can release antimicrobial and restorative Zn^{2+} in the uterus.

Although the contraceptive action of the bulk zinc was investigated by some researchers [11–13], the functions of zinc and zinc oxide nanoparticles have not been reported. Compared with zinc and zinc oxide bulk, zinc and zinc oxide nanoparticles show strong antibacterial activity [14]. Furthermore, the thromboresistant properties of zinc oxide nanoparticles are excellent [15], indicating that nanoparticles of zinc and zinc oxide may decrease the side effects of IUDs more effectively than their bulks.

The behavior of zinc and zinc oxide nanoparticles in simulated uterine solution (SUS) has been investigated in our previous work [16]. As a logical extension of our previous work, the main purpose of the present study was to investigate Zn^{2+} release and surface characteristics of the nanocomposites of zinc/low-density polyethylene (Zn/LDPE) and zinc-oxide/low-density polyethylene (ZnO/LDPE) in simulated uterine solution. Further studies concerning Zn^{2+} release of the nanocomposites may help us verify the feasibility of our composite system. This work may be valuable in providing the foundation for the application of Zn and ZnO nanoparticles in contraceptive.

2 Materials and methods

2.1 Materials

The polymeric matrix was a commercial low-density polyethylene (LDPE) in particle form, with a density of 0.93 g/cm^3 and a melt index of 2.5 g/min. Zinc and zinc oxide nanoparticles were provided by JUNYE nanomaterial Co. Ltd. in China. Zinc nanoparticles, about 30 nm across, agglomerated into larger particles of around 500 nm diameter. Zinc oxide nanoparticles were in a column shape with about 50 nm in diameter and 200 nm in length. The mean particle size of zinc microparticles and zinc oxide microparticles was about 40 μm and 0.2 μm, respectively.

2.2 Preparation of composite samples

Zn/LDPE composite and ZnO/LDPE composite with 15 wt.% nanoparticles were prepared by compressing molding. Nanocomposites were prepared by first mixing LDPE powders with nanoparticles in a tumble mixer to obtain a homogeneous mixture. Then the mixed powders were placed in a die and melted at 150°C under 4 MPa pressure. After cooling and solidification under 4 MPa pressure, the composite samples, in shape of column with 2.0 mm in diameter and 7.0 mm in length, were taken out of the die. For comparison, microcomposites with the same content of zinc and zinc oxide microparticles were prepared by using the same process.

In addition, in order to investigate the influences of preparation methods of nanocomposite on Zn^{2+} release, Zn/LDPE composite and ZnO/LDPE composite with 15 wt.% nanoparticles were prepared by hot-melt extrusing in a single-screw extruder at a screw speed of about 15–20 rpm. The temperature of the extruder was maintained at 145, 160, and 180°C from hopper to die, respectively.

2.3 Measurement of Zn^{2+} release rate

The simulated uterine solution was obtained by mixing the analytical grade chemicals of NaCl (4.97 g/l), KCl (0.224 g/l), $CaCl_2$ (0.167 g/l), $NaHCO_3$ (0.25 g/l), glucose (0.50 g/l), $NaH_2PO_4{\cdot}2H_2O$ (0.072 g/l) together. The pH value was kept at 6.5 by the addition of hydrochloric acid solution (analytical grade) or sodium hydroxide solution (analytical grade).

The samples with the same specific surface area were incubated in 50 ml of freshly prepared SUS at the temperature of 37 ± 0.2°C. After two days of incubation, Zn^{2+} concentrations in SUS were measured by absorbance measurements and Zn^{2+} release rate was calculated as μgZn/day. The samples were then putting back into the simulated uterine solution. The next measurement was carried out after an appropriate interval by using the same process.

2.4 Characterization of the microstructure of samples

The dissolution depth of ZnO/LDPE sample was analyzed by a SEM model Quanta-400 (manufactured by FEI of Holland) equipped with EDX elemental composition analyzer. The acceleration potential used during this investigation was 30 kV. Total scanning time during elemental map generation is 10 min. The composites were sputter coated with aurum to prevent charging when analyzed by the electron beam. The X-ray peaks generated during the scanning were used to record the elements present in the composites, and then elemental maps were generated. The images can show the distribution of each element on the composites.

The morphology and the composition of the sample surface were characterized by the same SEM/EDX model Quanta-400. The phase of the deposits on the sample surface was identified by a Rigaku D/max-3B X-ray diffractometer (XRD) using Nickel filtered Cu Kα radiation at a generator voltage of 30 kV and a generator current of

30 mA. The diffraction curves were obtained within the range of scattering angles (2θ) of 15–80° at a scan rate of 5°/min.

3 Results and discussion

3.1 The behaviour of Zn^{2+} release in SUS

3.1.1 The influences of sample preparation methods on Zn^{2+} release

Zn^{2+} release rates of the composites prepared by compressing molding and hot-melt extrusing were shown in Fig. 1a, b, respectively. From Fig. 1, it can be seen that Zn^{2+} release rates of the samples prepared by the compressing moulding and the hot-melt extrusing exhibit biphasic drug release behavior: an initial rapid release phase followed by a near zero-order release period.

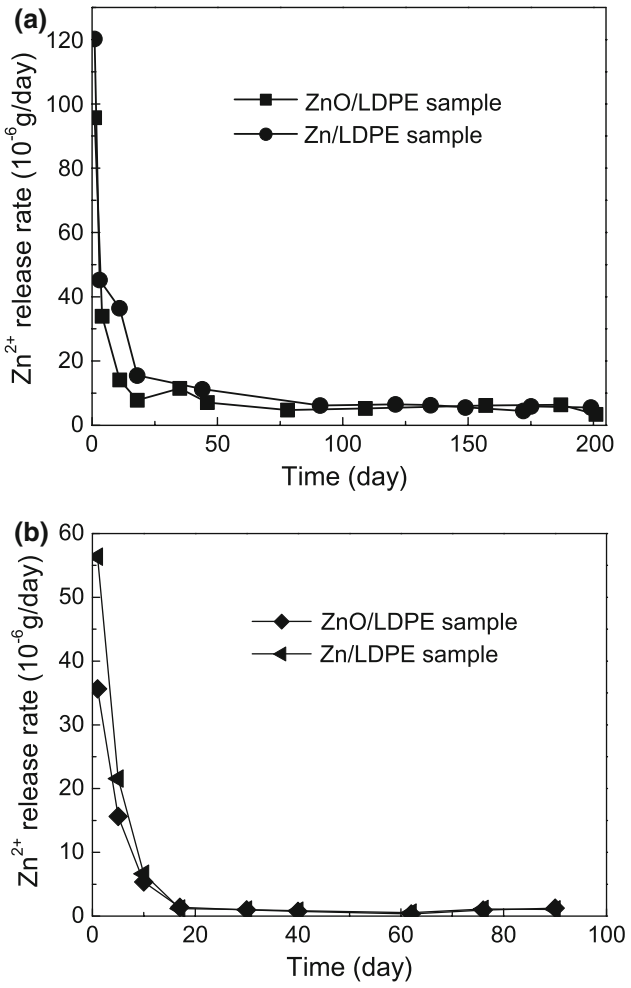

Fig. 1 Zn^{2+} release rates of the samples prepared by different preparation methods: (**a**) compressing moulding; (**b**) hot-melt extrusing

Furthermore, Zn^{2+} release rates of the samples prepared by compressing molding are about 2 times higher in the first few days and 4 times higher at the later stage than those of the samples prepared by hot-melt extrusing.

After Zn/LDPE nanocomposites and ZnO/LDPE nanocomposites are incubated in simulated uterine solution, zinc ions are released into SUS due to the dissolution of zinc and zinc oxide nanoparticles in the composites. Zn^{2+} release from the samples occurs primarily through a network of interconnected pores, which includes the intrinsic pore spaces associated with the matrix and the pores created by solid drug particles loaded in the matrix initially. Only through the interconnected pores can the reactants in the SUS reach the nanoparticles in LDPE composites to initiate the dissolution and the generated Zn^{2+} can diffuse outward [17]. With the dissolution of zinc and zinc oxide in the matrix, the porous region of the matrix grows at the expense of the undissolved drug-polymer region.

The rapid release rate of Zn^{2+}, which occurs mainly during the first 11 days, is attributed to the dissolution of nanoparticles attached on the sample surface. The reactants in SUS react with the nanoparticles at the sample surface directly and the generated Zn^{2+} enters into SUS without diffusion in the pores channels. The dissolution of nanoparticles at the surface would create the micropores, which provides the release pathway for the dissolution of the inner imbedded nanoparticles.

The appropriate rapid rate of Zn^{2+} release in the first few days may effectively help healing the uterus injury and killing the bacteria resulting from IUDs insertion, indicating that the side effects such as pain, bleeding and pelvic inflammatory disease that occurred mainly within the first month following IUDs insertion are hopeful to be reduced.

After the dissolution of nanoparticles at the surface, the release rate reaches a near zero-order release phase in the later stage with the dissolution of deep imbedded nanoparticles. The appearance of zero-order release periods in the release profiles obtained from inert matrix systems was theoretically predicted by Gumy et al. [18] and experimentally demonstrated by Caraballo et al. [19]. According to the literature [20], zero-order release periods in the release profiles are obtained when there is a saturation of drug into the water filled pores of the matrix.

In addition, from Fig. 1, it is interesting to note that Zn^{2+} release rates of the samples prepared by compressing molding are much higher than those of the samples prepared by hot-melt extrusing. This is consistent with the reported findings that sustained release dosage forms prepared by hot-melt extrusing have slower drug release rates than those prepared by traditional methods [21]. Compared with the sample prepared by compressing molding, the composite prepared by hot-melt extrusing shows a low porosity and a high tortuosity because the air present in the

powder bed is excluded from the polymer melt under much higher pressures during the processes of hot-melt extrusing [22]. The low porosity and high tortuosity of the composites are responsible for the low release rate of Zn^{2+}.

3.1.2 *The effects of particle size of zinc and zinc oxide on Zn^{2+} release*

Figure 2 shows Zn^{2+} release rates of the composite samples with nanoparticles and microparticles. From Fig. 2, the following trends can be seen that: compared with the microcomposites, the release profiles of the nanocomposites show a sharp decrease in Zn^{2+} release rate in the first 18 days, an early onset of a near zero-order release and a slightly low release rate of Zn^{2+} at the later stage.

As seen from Fig. 2, the release rates of the nanocomposites decrease significantly in the first 18 days. It can be explained that there is a high reaction rate for zinc and zinc oxide nanoparticles in SUS due to the large specific surface and high activity, resulting in the rapid dissolution of zinc and zinc oxide nanoparticles attached on the sample surface. As a result, the nanoparticles at the sample surface can dissolve in a shorter time, which leads to the sharp decrease in Zn^{2+} release rate.

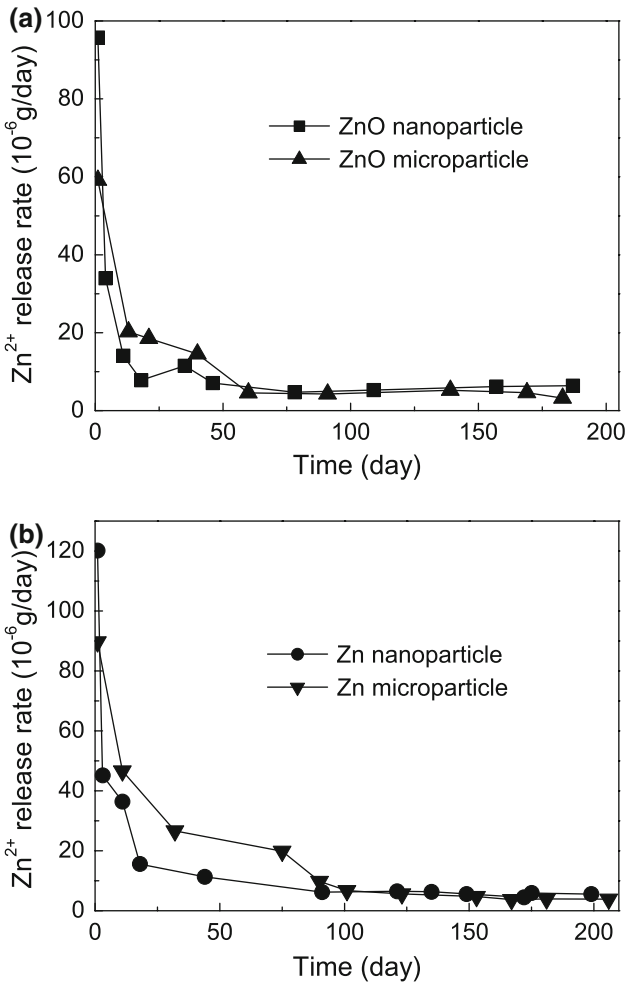

Fig. 2 The effects of particle size of zinc and zinc oxide on Zn^{2+} release rates of the samples: (**a**) ZnO/LDPE samples; (**b**) Zn/LDPE samples

Caraballo et al. [19] found that a minor particle results in an early onset of the zero-order release period. Especially, Isidoro Caraballo [20] found that the matrix with the large drug particle size did not exhibit clear zero-order release periods during the release assay. He believed that this fact could be attributed to the formation of great pores in matrix when the drug particles were dissolved. The saturation of drug cannot be clearly reached inside these large pores. In our work, it also can be seen that the increase of particle size delays the onset of the near zero-order release periods. For microcomposites, the low dissolution rate of microparticles and the large pores generated prolong the time to establish conditions of saturation in the aqueous filled pores, which delays the onset of zero-order periods.

In addition, Mónica Millán [23] found that the release rate of drug decreased with increasing drug particle size, which is also identified in our work. Zn^{2+} release rates of the nanocomposites are slightly higher than those of the microcomposites during the near zero-order period as shown in Fig. 4. Mónica Millán employed Higuchi's kinetic model [24] to explain the effect of the drug particle size on the drug release.

$$Q = a + bt^{1/2}$$

where Q is the amount of drug released after time per unit exposed area, and a, b are constants where b is Higuchi's slope. For the tablets prepared by traditional compression, he established the direct relation between the Higuchi's slope and the drug particle size with larger particle sizes corresponding to lower Higuchi's slope values, suggesting that the amount of drug release decreases with drug particle size increasing. Consequently, the release rates of the microcomposite samples are lower than those of nanocomposite samples.

3.2 The cross-section characterization of ZnO/LDPE sample

To further characterize the dissolution behavior of the nanoparticles in the matrix, SEM-EDX technique was employed to image the cross-section of nanocomposite. Peak intensities for elements carbon, oxygen and zinc were observed and recorded during the scanning of the samples. SEM-EDX mapping of the cross-section of ZnO/LDPE sample after incubation for 200 days are shown in Fig. 3. White dots indicate the presence of a specific element on the composite and black indicates the absence of an

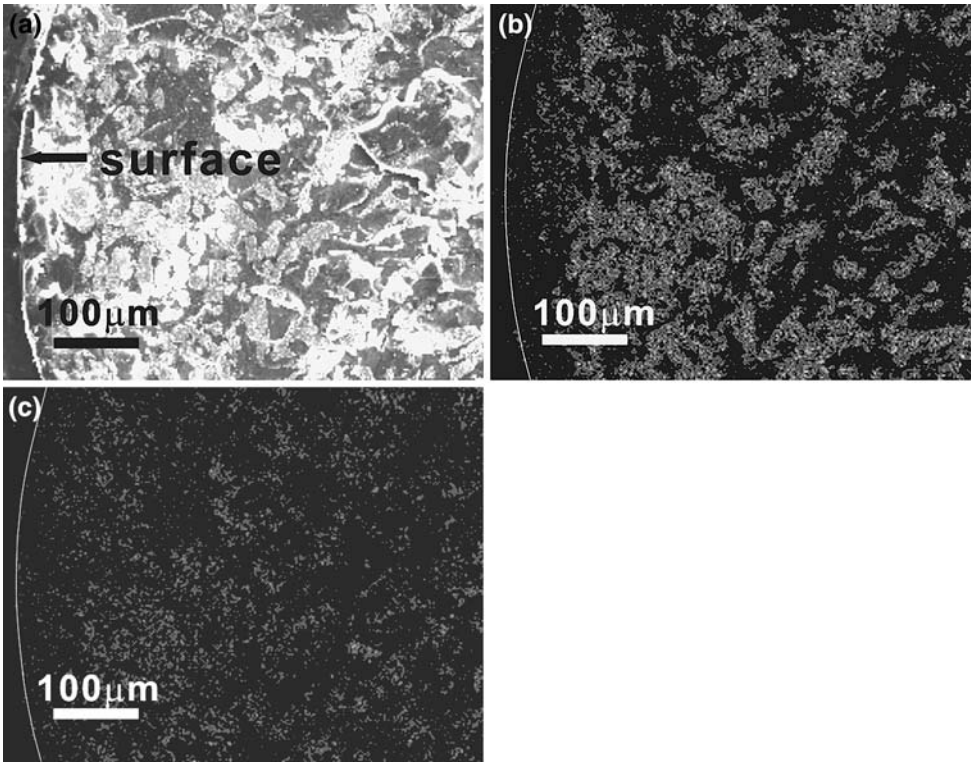

Fig. 3 SEM-EDX mapping of cross-section of ZNO/LDPE sample incubated for 200 days: (**a**) SEM image; (**b**) the corresponding EDX mapping of zinc; (**c**) the corresponding EDX mapping of oxygen. Arrow indicates the side of sample incubated

element. Figure 3 indicates that ZnO nanoparticles distribute non uniformly in LDPE matrix before incubation, indicating that ZnO nanoparticles have not been homogeneously mixed with LDPE powders during the process of sample preparation. From Fig. 3b, c, it can be seen that the concentration of zinc and oxygen increases gradually from surface toward the inner part of sample, suggesting that dissolution depth increases as time passed. The dissolution depth is about 60 μm in the composite after incubation for about 200 days, predicating that it is possible to keep sustained-release of zinc ions for more than 5 years.

3.3 The surface characteristics of the samples

3.3.1 The surface characteristics of ZnO/LDPE sample

The images of the surface of ZnO/LDPE sample before and after incubation were observed by SEM technique. Figure 4a indicates that ZnO nanoparticles at the surface distribute not very homogenously in LDPE matrix. Figure 4b shows that after incubation for 200 days, the unwanted deposits are not observed whereas a lot of pores are detected on the sample surface. The formation of these pores is attributed to the dissolution of the zinc oxide nanoparticles at the surface of the sample. The pores play a role as "channels" for the dissolution of ZnO nanoparticles deep inside the matrix.

To further investigate whether the undesirable deposit has formed on the sample surface or not, EDX technique was used to identify the chemical composition of the sample surface. SEM and EDX spectra of the surface of ZnO/LDPE sample after incubation is presented in Fig. 5. According to the literatures [25, 26], P, Na, and Ca signals have been identified on the surface of conventional IUDs after incubation in SUS by using EDX technique. However, those elements, which compose of the usual deposits, have not been detected on the surface of the ZnO/LDPE nanocomposite.

For conventional IUDs, the formation of those deposits increases the incidence of side effects such as abdominal complaints, bacterial and fungoid infections and concomitant inflammatory complications [27, 28]. However, no deposit forms on the surface of ZnO/LDPE nanocomposite. It may be explained that only LDPE remains when zinc oxide nanoparticles at the surface dissolve into SUS after the first few days. The poor wettability of LDPE prevents the usual insoluble matters like calcite and phosphates adhering to the sample surface. Therefore, the side effects caused by the formation of the deposits would be eliminated for IUDs made of the ZnO/LDPE nanocomposite.

3.3.2 The surface characteristics of Zn/LDPE samples

The surface images of Zn/LDPE sample before and after incubation are shown in Fig. 6. Similar to the surface

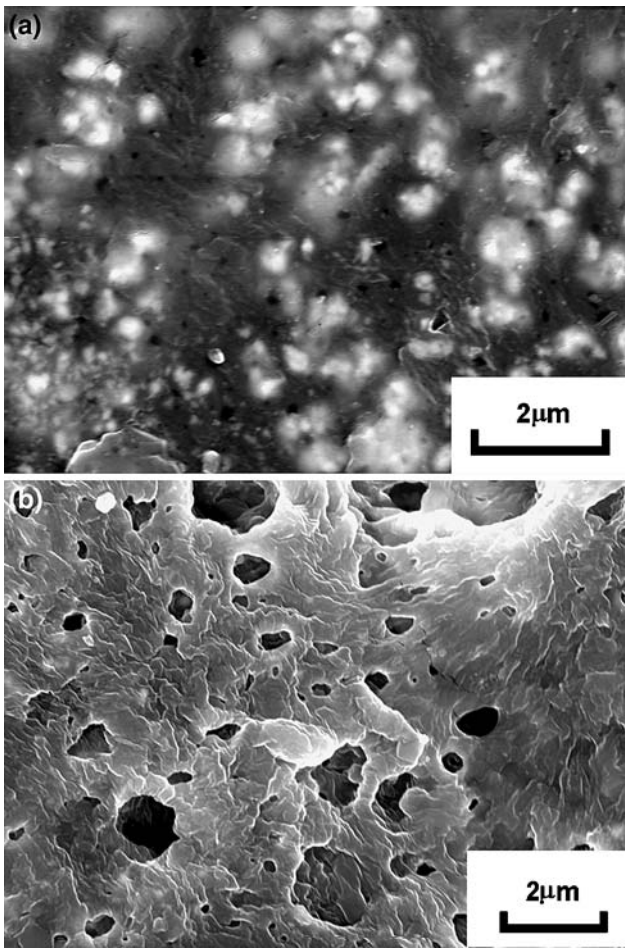

Fig. 4 SEM images of the surface of ZnO/LDPE sample before and after incubation: (**a**) before incubation; (**b**) after incubation for 200 days

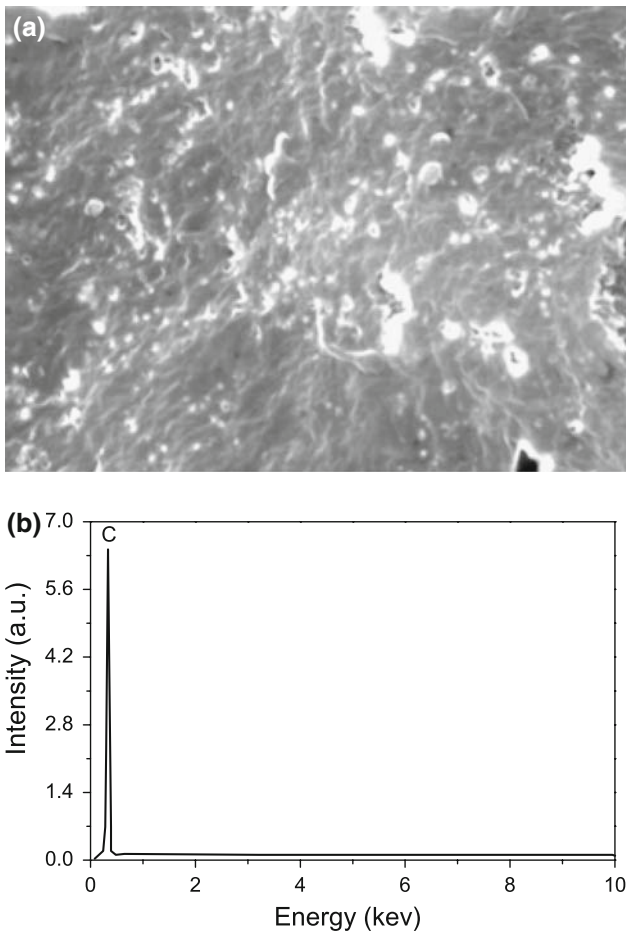

Fig. 5 SEM and EDX spectra of the surface of ZnO/LDPE sample after incubation for 200 days: (**a**) SEM image; (**b**) EDX spectra

image of ZnO/LDPE samples, the pores form on the surface of Zn/LDPE sample after incubation for 200 days due to the dissolution of Zn nanoparticles attached on the surface. The size of pores on the Zn/LDPE sample is smaller than that of pores on the ZnO/LDPE sample, which might be attributed to the formation of the deposits around the pores. The white deposits on the surface of Zn/LDPE sample can be observed with the naked eye after incubation.

EDX technique was employed to investigate the chemical compositions of the Zn/LDPE sample surface, and SEM image and EDX spectra of the sample surface are shown in Fig. 7. The results indicate that only carbon, zinc and oxygen elements are identified, and P, Cl, and Ca signals that compose of the deposits on the conventional IUDs have not been determined either.

XRD technique was employed to further determine the compounds that deposited on the surface of the Zn/LDPE sample. Figure 8 shows the XRD patterns of the Zn/LDPE sample after incubation for 200 days. It can be seen that the deposits on the surface are ZnO, the corrosion product of Zn. Other possible corrosion products of zinc like $Zn(OH)_2$ and $Zn_5(OH)_8Cl_2$ are not observed. At the same time, the usual deposits such as calcite and calcium phosphate on conventional IUDs surface are not detected either. The main possible reactions of ZnO formation in SUS take place as follows:

$$Zn + H_2O \rightarrow ZnO + 2H^+ + 2e$$

The formation of ZnO in solution occurs through a dissolution-precipitation mechanism. The active dissolution of zinc involves two consecutive one-electron charge transfer reactions with Zn^+ as intermediate, followed by the formation of Zn^{2+} ions. The Zn^{2+} produced can undergo a complexation reaction with water to yield ZnO_2^{2-} ions until a critical concentration is reached at which ZnO precipitates [29]. Zinc oxide precipitates on the surface of zinc substrate at the sample surface and grows into large particles slowly, which leads to deposit formation and reduces the pore size on the surface. This kind of deposits may increase the incidence of side effects of IUDs.

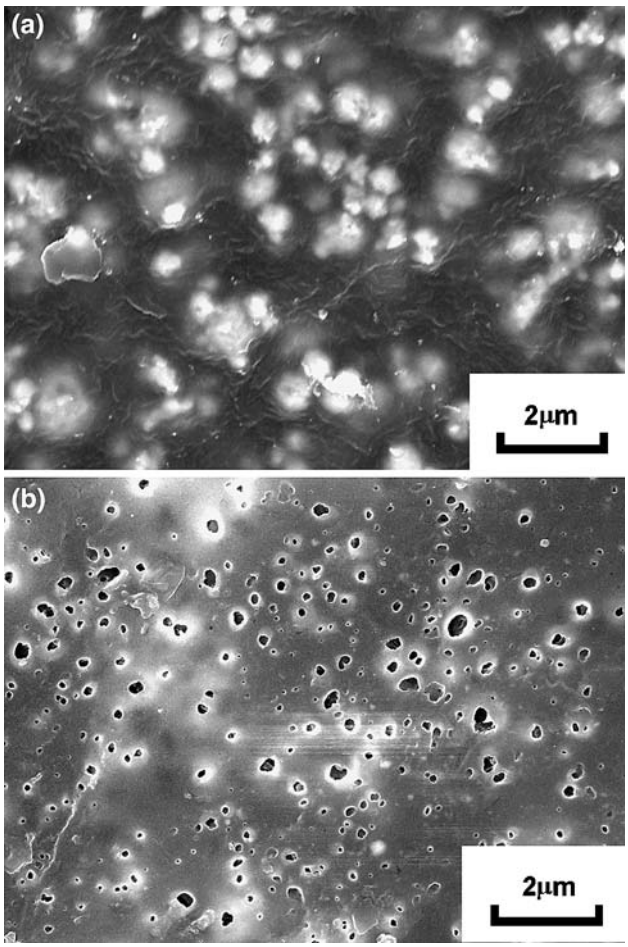

Fig. 6 SEM images of the surface of Zn/LDPE sample before and after incubation: (**a**) before incubation; (**b**) after incubation for 200 days

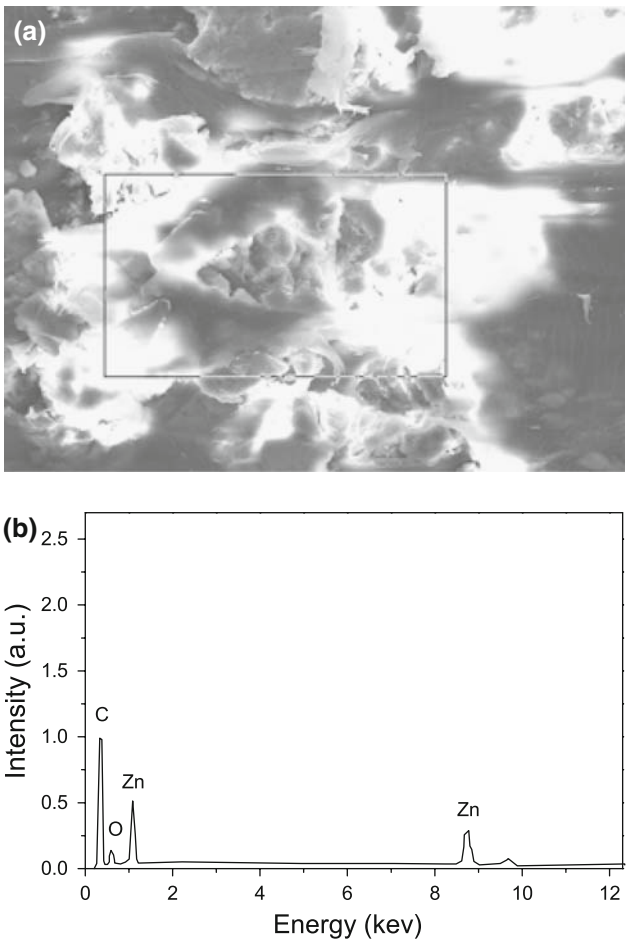

Fig. 7 SEM and EDX spectra of the surface of Zn/LDPE sample after incubation: (**a**) SEM image; (**b**) EDX spectra

4 Conclusions

Zn/LDPE nanocomposite and ZnO/LDPE nanocomposite were prepared with the mass fractions of 15 wt.% nanoparticles. Zn^{2+} release from the composite samples was investigated by changing the preparation methods of composites and the particles sizes of zinc and zinc oxide. The release profiles of all the samples show that the near zero-order release phases followed the rapid release phases. Zn^{2+} release rates of the samples prepared by compressing molding are much higher than those prepared by hot-melt extruding. The release profiles of the nanocomposites show a sharp decrease of Zn^{2+} release rate in the first 18 days due to the rapid dissolution of the nanoparticles at the sample surface. Compared with microparticles, the nanoparticles bring forward the onset of the near zero-order period and increase Zn^{2+} release rate of the composites at the later stage.

After incubation in SUS for 200 days, the dissolution depth of ZnO/LDPE nanocomposite is about 60 μm, predicating that the ZnO/LDPE nanocomposite can keep

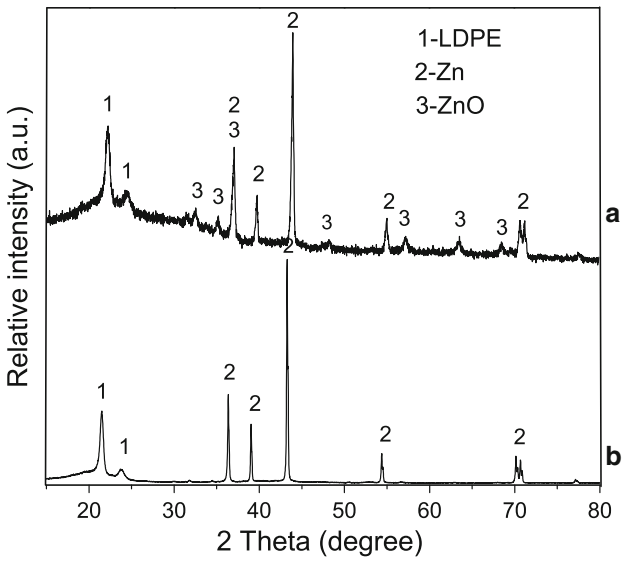

Fig. 8 XRD patterns of Zn/LDPE sample before and after incubation: (a) after incubation for 200 days; (b) before incubation

sustained-release of Zn^{2+} for more than 5 years. The surface of ZnO/LDPE and Zn/LDPE samples after incubation is full of pores that provide the pathways for the dissolution of the particles in the matrix. The undesirable deposit has not been found on the surface of ZnO/LDPE nanocomposite, but it has been observed on the surface of Zn/LDPE nanocomposites. The deposit, the corrosion product of zinc, is zinc oxide. These results indicate that the ZnO/LDPE nanocomposites would alleviate the side effects of IUDs more effectively than the Zn/LDPE nanocomposite.

Acknowledgements The authors gratefully acknowledge the financial support by National Natural Science Foundation of China (NFSC, Grant No. 50671039 and 50271029) and Natural Science Foundation of China University of Geosciences (Grant No. CUGQNL0521).

References

1. E.A. Wright, A.O. Aisien, Int. J. Gynecol. Obstet. **28**, 133 (1989)
2. D.A. Grimes, Contraception. **36**, 97 (1987)
3. B. Dahlberg, S. Kullander, J. Ursing, A. Forsgren, Contraception **20**, 71 (1979)
4. M. Toppozada, Contraception **36**, 145 (1987)
5. E.C. Yeiser, A.A. Lerant, R.M. Casto, C.W. Levenson, Neurosci. Lett. **277**, 75 (1999)
6. P.W. Jones, D.W. Taylor, D.R. Williams, J. Inorg. Biochem. **81**, 1 (2000)
7. P.W.R. Osinaga, R.H.M. Grande, R.Y. Ballester, M.R.L. Simionato, C.R.M.D. Rodrigues, A. Muench, Dent Mater **19**, 212 (2003)
8. A. Top, S. Ulku, Appl. Clay Sci. **27**, 13 (2004)
9. M.D.K. Hagenfeldt, Contraception **6**, 37 (1972)
10. B. Daunter, E.M. Chantler, M. Elstein, Contraception **15**, 543 (1977)
11. J. Zipper, M. Medel, R. Prager, Am. J. Obstet. Gynecol. **105**, 529 (1969)
12. M. Medel, C. Espinoza, J. Zipper, R. Prager, Contraception **6**, 241 (1972)
13. W.L. Williams, Contraception **22**, 659 (1980)
14. O. Yamamoto, Int. J. Inorg. Mater. **3**, 643 (2001)
15. C. Li, G.D. Hu, Y.H. He, Chin. J. Pro. Eng. **3**, 34 (2003)
16. Z.H. Yang, C.S. Xie, Colloids Surf. B. **47**, 140 (2006)
17. S.Z. Cai, X.P. Xia, C.S. Xie, Biomaterials. **26**, 2671 (2005)
18. R. Gumy, E. Doelker, N.A. Peppas, Biomaterials. **3**, 27 (1982)
19. I. Caraballo, M. Fernández-Arévalo, M.A. Holgado, A.M. Rabasco, Int. J. Pharm. **96**, 17 (1993)
20. I. Caraballo, M. Millán, A.M. Rabasco, H. Leuenberger, Pharm. Acta. Helv. **71**, 335 (1996)
21. C.R. Young, J.J. Koleng, J.W. Mcginity, Int. J. Pharm. **242**, 87 (2002)
22. M.M. Crowley, B. Schroeder, A. Fredersdorf, S. Obara, M. Talarico, S. Kucera, J.W. Mcginity, Int. J. Pharm. **269**, 509 (2004)
23. M. Millán, I. Caraballo, Int. J. Pharm. **310**, 168 (2006)
24. T. Higuchi, J. Pharm. Sci. **52**, 1145 (1963)
25. J.M. Bastidas, E. Cano, N. Mora, Contraception **61**, 395 (2000)
26. K. Patai, L. Dévényi, R. Zelkó, Contraception **70**, 149 (2004)
27. M. Rizk, N. Shaban, I. Medhat, Y.M.E. Dien, M.A. Ollo, Contraception **42**, 643 (1990)
28. K. Patai, M. Berényi, M. Sipos, B. Noszál, Contraception **58**, 305 (1998)
29. E.E.F. El-sherbini, S.S.A. El-rehim, Corros. Sci. **42**, 785 (2000)